A climatic evaluation of the southern dispersal route during MIS 5e

Nicholson, S. L. ORCID: https://orcid.org/0000-0002-6760-0321, Hosfield, R. ORCID: https://orcid.org/0000-0001-6357-2805, Groucutt, H. S. ORCID: https://orcid.org/0000-0002-9111-1720, Pike, A. W. G., Burns, S. J., Matter, A. and Fleitmann, D. (2022) A climatic evaluation of the southern dispersal route during MIS 5e. Quaternary Science Reviews, 279. 107378. ISSN 02773791 doi: 10.1016/j.quascirev.2022.107378 Available at https://centaur.reading.ac.uk/102625/

Quaternary Science Reviews 279 (2022) 107378

Contents lists available at ScienceDirect

Quaternary Science Reviews

journal homepage: www.elsevier.com/locate/quascirev

A climatic evaluation of the southern dispersal route during MIS 5e

Samuel Luke Nicholson [a, b, *], Rob Hosfield [b], Huw S. Groucutt [c, d, e], Alistair W.G. Pike [f], Stephen J. Burns [g], Albert Matter [h], Dominik Fleitmann [b, i, **]

[a] Ecology and Evolutionary Biology, University of Reading, Reading, RG6 6LA, United Kingdom
[b] Department of Archaeology, University of Reading, Reading, RG6 6AB, United Kingdom
[c] Extreme Events Research Group, Max Planck Institute for Chemical Ecology, 07745, Jena, Jena, Germany
[d] Department of Archaeology, Max Plank Institutes for Chemical Ecology, The Science of Human History, and Biogeochemsitry, 07745, Jena, Germany
[e] Institute of Prehistoric Archaeology, University of Cologne, Cologne, 5093, Germany
[f] Department of Archaeology, University of Southampton, Southampton, SO17 1BF, United Kingdom
[g] Department of Geosciences, University of Massachusetts, MA, 01003-9297, United States
[h] Institute of Geophysics, University of Bern, CH-3012, Bern, Switzerland
[i] Department of Environmental Sciences, University of Basel, CH-4056, Basel, Switzerland

ARTICLE INFO

Article history:
Received 16 March 2021
Received in revised form
17 December 2021
Accepted 10 January 2022
Available online 24 January 2022

Handling Editor: Dr Giovanni Zanchetta

Keywords:
Human dispersal
Arabia
Monsoon
Pleistocene
MIS 5e

ABSTRACT

Homo sapiens dispersals out of Africa are often linked to intensifications of the African and Indian Summer Monsoons. Current models advocate that dispersals along the "southern-route" into Arabia occurred during Glacial Termination-II (T-II), when lower sea-level and reduced Bab-al-Mandab width increased the likelihood of crossing. The precise phasing between sea-level and monsoon precipitation is thus key to assess the likelihood of a successful crossing or the behavioural and technological capacities that facilitated crossing. Based on a precisely-dated stalagmite record from Yemen, we reveal a distinct phase-lag of several thousand years between sea-level rise and major monsoon intensification. Pluvial conditions in Southern Arabia during MIS 5e lasted from ~127.7 to ~121.1 ka BP and occurred when sea-levels were already higher than at present. Based on our observations, we propose three models for the dispersal of *H. sapiens* which all have pertinent implications for our understanding of human technological and behavioural capacities during MIS 5e.

1. Introduction

Understanding how *H. sapiens* spread from Africa across the world is one of the most debated topics in human evolution (Mellars et al., 2013; Groucutt et al., 2015a; Bae et al., 2017). Two proposed main dispersal routes cross Arabia: a northern-route across the Sinai into the Levant and a southern-route from the Horn of Africa via the Strait of Bab-al-Mandab into Southern Arabia and beyond (Fig. 1). The accessibility of these entry points was spatiotemporally variable and related to major climatic changes across the Saharo-Arabian deserts. During interglacial periods, both the African and Indian Summer Monsoons (ASM and ISM, respectively) were much stronger, expanded northward and transformed the Saharo-Arabian deserts into green landscapes for a few millennia (Fleitmann et al., 2003b; Parton et al., 2015a; Petraglia et al., 2015; Tierney et al., 2017; Nicholson et al., 2020; Menviel et al., 2021). These pluvial periods, termed "Green Arabia Periods" and "South Arabian Humid Periods" (SAHPs), provided optimal periods for *H. sapiens* to disperse from sub-Saharan Africa into Eurasia (Fleitmann et al., 2011; Rosenberg et al., 2011; Larrasoaña et al., 2013; Nicholson et al., 2020). Over the last 130 ka BP, pluvial conditions in Southern Arabia occurred during Marine Isotope Stages (MIS) 5 and 1, and lasted from ~128 to 121 ka BP (MIS 5e; SAHP 4), ~104–97 ka BP (MIS 5c; SAHP 3) and ~84–71 ka BP (MIS 5a; SAHP 2) and ~10.5 to 6.2 ka BP (SAHP 1) (Fleitmann et al., 2011; Nicholson et al., 2020), and perhaps between 60 and 50 ka BP (onset of MIS 3) (McLaren et al., 2009; Parton et al., 2013, 2018).

The southern dispersal route involves a maritime crossing of the Bab-al-Mandab Strait. However, its current width of approximately

* Corresponding author. Ecology and Evolutionary Biology, University of Reading, Reading, RG6 6LA, United Kingdom.
** Corresponding author. Department of Environmental Sciences, University of Basel, CH-4056, Basel, Switzerland.
E-mail addresses: sam.nicholson@reading.ac.uk (S.L. Nicholson), dominik.fleitmann@unibas.ch (D. Fleitmann).

https://doi.org/10.1016/j.quascirev.2022.107378
0277-3791/

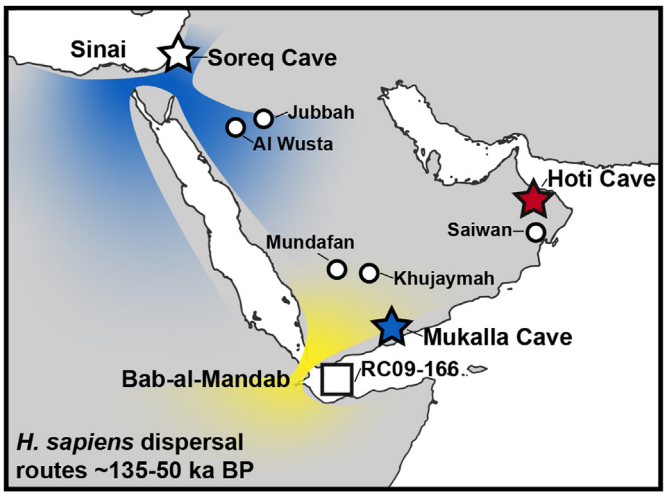

Fig. 1. Map of Arabia with locations of Mukalla Cave (blue star), Hoti Cave (red star), Soreq Cave (white star), palaeolakes (white circles), RC09-166 (white square) and proposed *H. sapiens* northern (blue) and southern (yellow) entry points into Arabia (Armitage et al., 2011; Rohling et al., 2013; Petraglia et al., 2019; Beyer et al., 2021). (For interpretation of the references to colour in this figure legend, the reader is referred to the Web version of this article.)

~26 km represents a significant challenge to dispersal and was more likely traversable at times of lower sea-level, especially if seafaring technologies were limited. One proposed timing for early *H. sapiens* dispersals is Glacial Termination-II (T-II), between 136–129 ka BP, when sea-levels were lower than today and the width of the Bab-al-Mandab Strait (BaM_{width}) was reduced to a few kilometres (Armitage et al., 2011; Lambeck et al., 2011). From a palaeoclimatic perspective, a dispersal was most likely to have occurred at times of increased precipitation and biomass across Arabia (Groucutt et al., 2015a, 2018; Parton et al., 2015b). However, several lines of evidence point to a phase-lag of several thousand years between sea-level rise and northward migration of the monsoonal rainbelt due to colder northern-hemisphere temperatures related to Heinrich Stadial (HS) 11 between 135 and 130 ka BP (Cheng et al., 2009; Böhm et al., 2015; Häuselmann et al., 2015; Marino et al., 2015). In other words, arid conditions may have prevailed in Arabia during T-II, forming a biogeographical barrier to widespread dispersals despite low sea-levels. Establishing the precise phasing between sea-level change and ASM/ISM intensification during the MIS 6-5e transition from palaeoclimate records close to the Bab-al-Mandab Strait, with precise and accurate chronologies, is one critical factor for understanding accessibility of the southern dispersal route. Here, we present a precisely-dated and highly-resolved speleothem-based climate record from Mukalla Cave in Yemen, covering MIS 5e (SAHP 4: Nicholson et al., 2020). Precise Uranium-series (^{230}Th) ages allow us to evaluate the temporal phasing between ASM/ISM rainfall and sea-level change at a possible point-of-entry into Southern Arabia.

2. Environmental settings, materials and methods

Stalagmite Y99 was collected from Mukalla Cave (14°55′02″N; 48°35′23″ E; ~1500 masl; Fig. 1) in southern Yemen, where climate is strongly governed by the ASM and ISM. At present, both Mukalla Cave and the Bab-al-Mandab Strait are located at the northern and north-eastern margins of the ASM and ISM, with rainfall averaging <150 mm yr^{-1} (Fleitmann et al., 2011). Stalagmite Y99 extends back to 1.1 million years and was deposited in 17 punctuated growth intervals, with Growth Interval-I (GI-I) being the youngest and dated to MIS 5e (Nicholson et al., 2020). Previous analysis of Y99 was focussed on the broad timing and climatic conditions (bulked $\delta^{18}O$ and $\delta^{13}C$ isotope analysis) of SAHPs over the last 1.1 million-years (Fleitmann et al., 2011; Nicholson et al., 2020). Here, we provide high-resolution records and a focussed study of the timing of SAHP 4 compared to sea-level. We used the StalAge algorithm to calculate a robust age-model from previously collected ^{230}Th ages. This was then used to provide $\delta^{18}O_{ca}$ (ASM and ISM rainfall) and $\delta^{13}C_{ca}$ records at <100 years resolution.

The width of the Bab-al-Mandab Strait (BaM_{width}) was reconstructed using bathymetry data and the Red Sea relative sea-level (RSL) curve. The RSL has been constructed using marine core $\delta^{18}O_{G.\ ruber}$ records from the Red Sea which were combined with exposed coral terraces (Siddall et al., 2003; Rohling et al., 2008, 2009). The chronology of the RSL time-series is based on correlations with Mediterranean Core LC21 and the revised ^{230}Th chronology of the Soreq Cave record for periods younger than 150 ka BP to create a series of age tie-points (Rohling et al., 2009; Grant et al., 2012, 2014). Grant et al. (2014) then interpolated a 2σ chronological uncertainty from the tie-points to RSL data points and combined with methodological sea-level uncertainties to create a probabilistic assessment of the RSL. Using a local sea-level record that exploits a basin isolation effect means that our assessment is unaffected by isostatic effects, allowing us to compare regional climates with sea-level variations that control the sill depth and the width of the Strait. Additionally, there has been negligible tectonic uplift along the Egyptian Red Sea coast over the course of the Late Pleistocene (Arvidson et al., 1994; Fig. 11), and tectonic deformation in the Red Sea was more important prior to the late glacial/interglacial cycle (Lambeck et al., 2011). Thus, our reconstructions of the Strait during MIS 5e did not consider the potential impacts of tectonic change. We used the freely available QGIS software package and 15 arc-second (~450 m between 12 and 14°N) interval elevation and bathymetry data (GEBCO Compilation Group, 2020) in combination with the RSL to estimate BaM_{width} over the last 150 kyrs (extended methods).

3. Results and discussion

3.1. Timing and duration of SAHP 4

The chronology of the MIS 5e section of stalagmite Y99 is based on seven ^{230}Th ages. Two ages were discarded: one ^{230}Th age at the top was not included as it is most likely influenced by condensation corrosion and one age appears to be an outlier for unknown reasons (extended methods; Figs. S1 and S2). Importantly, the onset of stalagmite growth is determined by two ^{230}Th ages of 127.634 ± 0.557 ka BP and 127.811 ± 0.626 ka BP; whereas the StalAge model places the onset of growth at 127.725 ± 0.448/0.374 ka BP. Stalagmite growth ceased at around 121.170 ± 0.500 ka BP (Fig. 2A). As ~300 mm yr^{-1} of rainfall are mostly likely required to trigger large speleothem growth in desert caves (Vaks et al., 2010), onset of stalagmite growth reveals that monsoonal rainfall during MIS 5e (SAHP 4) was at least twice as high as today. This threshold was established by the distribution of fossil and active stalagmite growth in the Negev Desert, where a winter precipitation regime permits a sufficient precipitation-evaporation (P-E) balance for stalagmite formation (Vaks et al., 2006, 2010). Conversely, monsoonal rainfall to Southern Arabia was delivered during the hot summer months (Nicholson et al., 2020). However, the summer monsoon season (locally known as the "Khareef") in Dhofar (Southern Oman) is characterised by low clouds and mists which reduce evaporation and permit the formation of ephemeral green landscapes. A simultaneous increase of rainfall and cloud cover across Southern Arabia during MIS 5e (Herold and Lohmann, 2009)

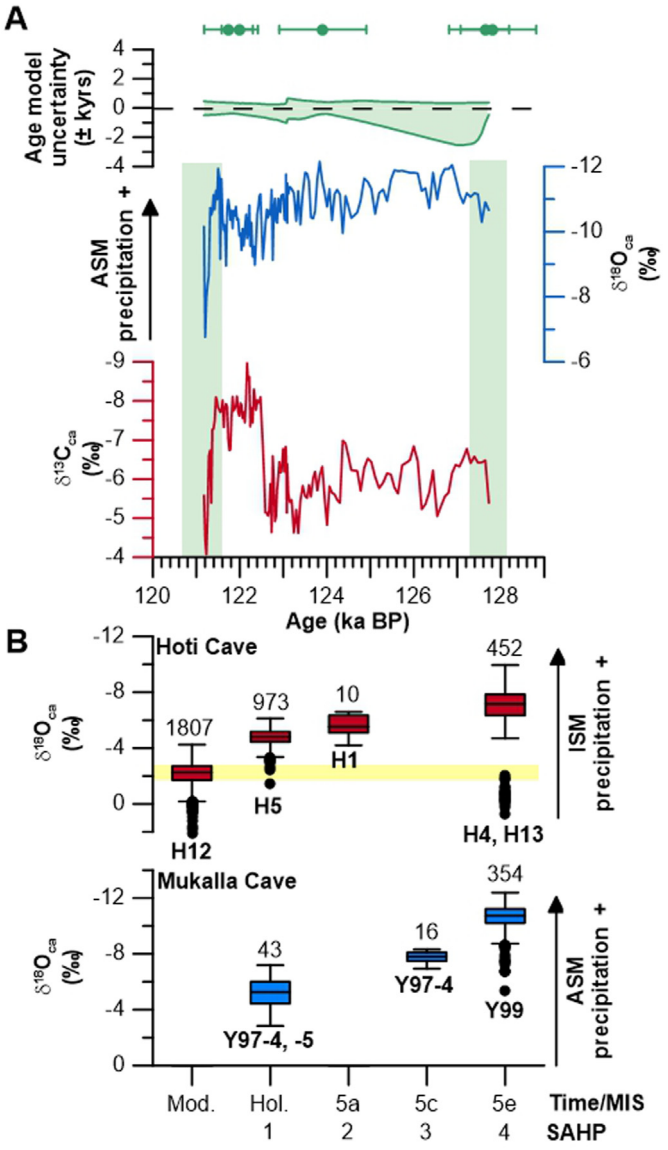

Fig. 2. A) ^{230}Th ages, StalAge model uncertainty, $\delta^{18}O_{ca}$ and $\delta^{13}C_{ca}$ values of GI-I (MIS 5e) of Y99. B) Box-whisker plot comparison of Hoti Cave (Oman) and Mukalla Cave (Yemen) stalagmite $\delta^{18}O_{ca}$ values from Fleitmann et al. (2011) and Nicholson et al. (2020). Numbers above and below box-whiskers indicate amount of $\delta^{18}O_{ca}$ measurements and speleothem samples, respectively. The yellow bar denotes the range of modern $\delta^{18}O$ values in Oman, derived mostly from winter rainfall. (For interpretation of the references to colour in this figure legend, the reader is referred to the Web version of this article.)

likely increased the P-E balance to facilitate stalagmite formation. We apply a 300 mm yr^{-1} threshold as a minimum, although the height and diameter of stalagmite Y99 and contemporaneously deposited speleothems in Hoti Cave in Northern Oman (Burns et al., 2001; Fleitmann et al., 2011) suggest annual rainfall must have been considerably higher (Burns et al., 2001). This assumption is supported by model-based estimates of rainfall over Arabia during MIS 5e (Otto-Bliesner, 2006; Herold and Lohmann, 2009; Jennings et al., 2015; Gierz et al., 2017). Based on the age model for stalagmite Y99, SAHP 4 lasted for ~6.5 kyrs, which is slightly longer than the 4.3 kyr-long Holocene Humid Period in Southern Arabia (Fleitmann et al., 2007, Fig. 3).

Additional evidences support the timing and duration of SAHP 4. The onset of the MIS 5e growth interval (SAHP 4) of stalagmite Y99 at 127.725 ± 0.448/0.374 ka BP is synchronous with the onset of sapropel S5 at ~128.3 ± 2 ka BP (Grant et al., 2017) and associated negative shifts in speleothem $\delta^{18}O_{ca}$ records from Soreq and Peqiin Caves in Israel (Bar-Matthews et al., 2003). In both caves, speleothem $\delta^{18}O_{ca}$ values are strongly influenced by the "source effect", as $\delta^{18}O$ of (palaeo)precipitation in the Levant is directly linked to $\delta^{18}O$ of surface water in the Eastern Mediterranean. During interglacial periods, increased monsoon precipitation in the Ethiopian Highlands and higher discharge of low-$\delta^{18}O$ freshwater runoff from the Nile and North African wadi systems (Grant et al., 2012) into the Mediterranean lead to more negative $\delta^{18}O$ and sapropel formation (Rohling et al., 2015). Thus, the sharp decrease in $\delta^{18}O_{ca}$ at ~128.3 ± 1.2 ka BP in the Soreq and Peqiin Cave records (Fig. 3) is caused by an up to ~8 times higher Nile flow (Amies et al., 2019) during MIS 5e. Taken together, the Soreq and Peqiin Cave records are in line with marked increase in ASM and ISM rainfall at onset of SAHP 4 at 127.725 ± 0.448/0.374 ka BP in stalagmite Y99, supporting the accuracy of its chronology. The termination of SAHP 4 at 121.170 ± 0.500 ka BP is also concurrent with the independently derived age estimate for the termination of sapropel S5 at ~121.5 ± 2 ka BP (Grant et al., 2016, 2017) and the distinct positive shift in $\delta^{18}O_{ca}$ in the Soreq and Peqiin Cave records (Bar-Matthews et al., 2003). Such a close correspondence between sapropel deposition in the Eastern Mediterranean and the timing of peak rainfall in Southern Arabia is also observed for other SAHPs (Nicholson et al., 2020) and (SAHP 1) between 10.5 and 6.2 ka BP (Fleitmann et al., 2007; Grant et al., 2017). The timing of SAHP 4 also conforms with significantly higher ASM/ISM rainfall in other monsoon records from the region (Weldeab et al., 2007; Grant et al., 2017; Tierney et al., 2017, Fig. 4).

3.2. Climatic and environmental conditions during SAHP 4

Fluctuations in $\delta^{18}O_{ca}$ from Mukalla Cave speleothems are related to changes in the amount of ASM precipitation in Yemen (Fleitmann et al., 2011; Nicholson et al., 2020). This is confirmed by isotope measurements (δD and $\delta^{18}O$) of stalagmite fluid inclusion water, showing that the ASM was the dominant moisture source at Mukalla Cave during MIS 5e (Nicholson et al., 2020). The $\delta^{18}O_{ca}$ profile of stalagmite Y99 shows three distinct features. Firstly, $\delta^{18}O_{ca}$ values are lowest at onset and during the first phase of SAHP 4, indicating that ASM rainfall increased rapidly at the onset of SAHP 4, likely within a few centuries and similar to ISM monsoon records from Southern Oman (Fleitmann et al., 2003a). Such a rapid increase of rainfall and stalagmite formation is supported by analogues with Holocene stalagmites H5 (Hoti Cave) and Q5 (Qunf Cave) from Oman (Fig. 3) which show a rapid increase in rainfall at the beginning of the Holocene (Fleitmann et al., 2007). Secondly, ASM rainfall is highest until ~124 ka BP and decreases following the 30°N summer insolation curve. Thirdly, the abrupt positive shift in $\delta^{18}O_{ca}$ at 121.170 ± 0.500 ka BP indicates an abrupt termination of SAHP 4, most likely within a few decades (Burns et al., 2001). This is a common feature of SAHPs (Nicholson et al., 2020) and related to the geographical location of the cave in relation to the position of the Intertropical Convergence Zone and monsoonal rainfall belt (Fleitmann et al., 2007). The abrupt termination of speleothem growth and positive isotopic shifts indicate a rapid retraction of the Intertropical Convergence Zone and associated monsoonal rainfall southwards of Mukalla Cave. In addition, Y99 SAHP 4 $\delta^{18}O_{ca}$ values show that monsoon precipitation was substantially higher during MIS 5e (SAHP 4) compared with subsequent SAHPs (Fig. 2B). This isotopic difference is also observed at Hoti Cave (Fleitmann et al., 2011; Nicholson et al., 2020, Fig. 2B). Overall, Y99 $\delta^{18}O_{ca}$ values indicate that MIS 5e saw the most substantial enhancement of monsoon precipitation during the Late Pleistocene.

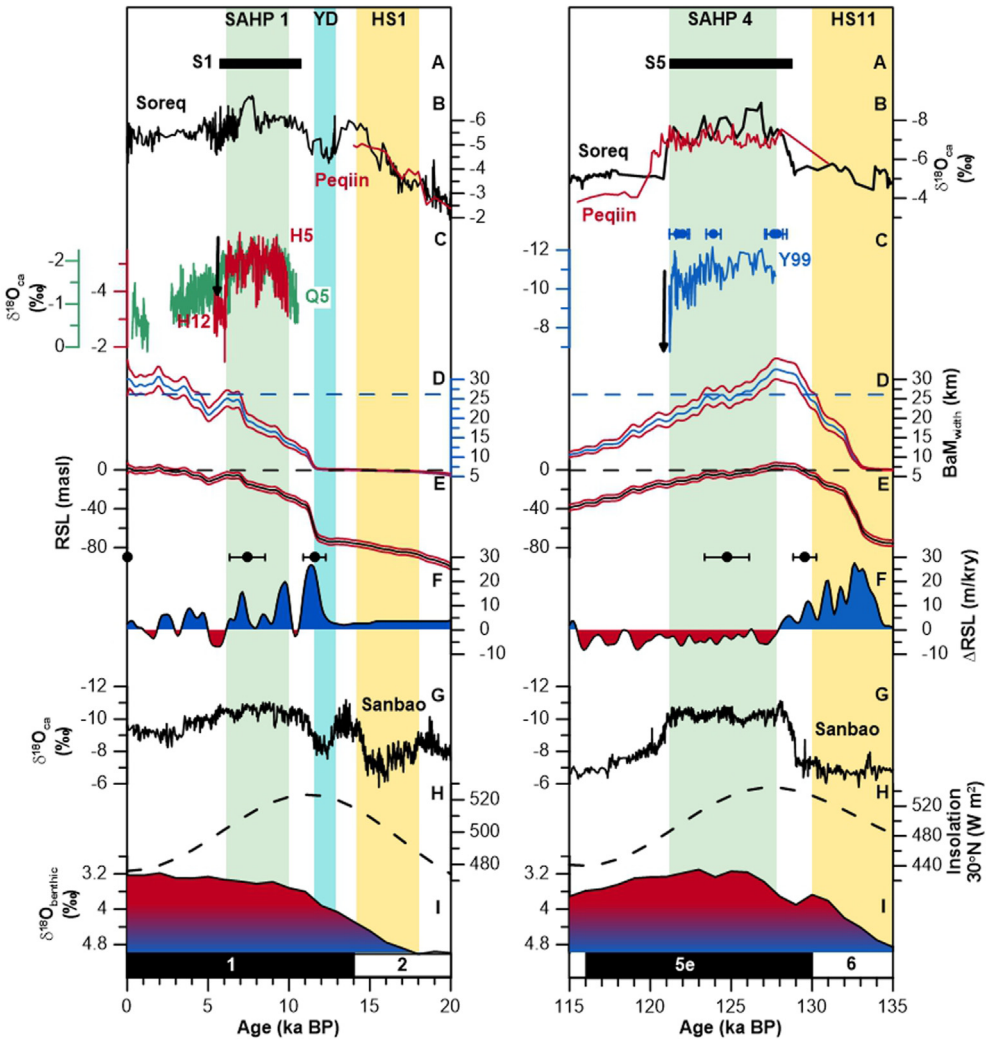

Fig. 3. (A) Duration of sapropel S1 and S5 (Grant et al., 2017). (B) Soreq and Peqiin cave $\delta^{18}O_{ca}$. (C) Holocene (H5, H12 and Q5) and MIS 5e (Y99) stalagmite $\delta^{18}O_{ca}$ records from Qunf Cave (green) (Fleitmann et al., 2003a), Hoti Cave (red) (Fleitmann et al., 2004, 2007) and Mukalla Cave (blue). (D) Reconstructed Bab-al-Mandab width using bathymetry data (GEBCO Compilation Group, 2020) and (E) the Relative sea-level (RSL) curve Probability-Maximum (Pmax; black), 95% confidence intervals (red) (Grant et al., 2012, 2014). (F) Rate of sea-level change predicted from RSL (Grant et al., 2012, 2014). Chronological uncertainties given by RSL component tie-points are given between E and F. (G) Sanbao Cave (China) composite stalagmite $\delta^{18}O_{ca}$ (Cheng et al., 2009, 2016). (H) July insolation (W m_2) at 30°N (Berger and Loutre, 1991, 1999). (I) Global ice-volume (LR04 $\delta^{18}O_{benthic}$) and Marine Isotope Stages (Lisiecki and Raymo, 2005). Green bars denote duration of SAHP 1 and 4, yellow bars denote timing of HS1 and HS11 and the blue bar denotes the timing of the Younger Dryas event. (For interpretation of the references to colour in this figure legend, the reader is referred to the Web version of this article.)

Stalagmite Y99 $\delta^{13}C_{ca}$ values are influenced by numerous factors, including vegetation type and density, and soil thickness and moisture above the cave (Nicholson et al., 2020). However, the various, and sometimes counteracting, controls means that stalagmite $\delta^{13}C_{ca}$ values can be difficult to interpret and the principal factors controlling $\delta^{13}C_{ca}$ values may change over time. Y99 $\delta^{13}C_{ca}$ values vary between −4.6 and −9.0‰ and thus fall into a mixed C_3/C_4 vegetation signal (Clark et al., 1997), suggesting that grasslands with some woody cover were present above Mukalla Cave during SAHP 4. This is consistent with palaeontological records across Arabia and phytolith records from Jebel Faya (MIS 5e) and Mundafan (MIS 5c/5a), indicating that now arid areas of Arabia were characterised by grasslands and some woody cover during wetter periods (Rosenberg et al., 2011, 2013; Bretzke et al., 2013; Groucutt et al., 2015c). Similar to the Y99 $\delta^{18}O_{ca}$ profile, the termination of stalagmite growth is characterised by an abrupt increase in $\delta^{13}C_{ca}$ (Fig. 2A) as rainfall, drip-rate and vegetation density decreased rapidly above Mukalla Cave.

3.3. Phasing between pluvial conditions in Southern Arabia and sea-level change during MIS 5e

Based on the stalagmite Y99 stable isotope records, climatic and environmental conditions in Southern Arabia were generally favourable for human dispersal along the southern dispersal route during MIS 5e. A key-question is therefore whether BaM_{width} was narrow enough for a successful crossing into Arabia during MIS 5e and SAHP 4.

The absolute and precise age-models for the MIS 5e (SAHP 4) growth interval of stalagmite Y99 allows the comparison of the phasing between monsoonal rainfall, the RSL and BaM_{width} (Fig. 3). Based on chronological uncertainties of the RSL, sea-levels at the Hanish Sill were higher than present between 126 and 130 (95% confidence limits of RSL Pmax) or 120–133 ka BP (RSL data points), and peaked between 127 and 129 (95% confidence limits of RSL Pmax) or 126–132 ks BP (RSL data points) (Grant et al., 2014). The onset of SAHP 4 at 127.725 ± 0.450/0.370 ka BP occurred when sea-level was already 4.7 ± 3.9 m higher than today and the width of the

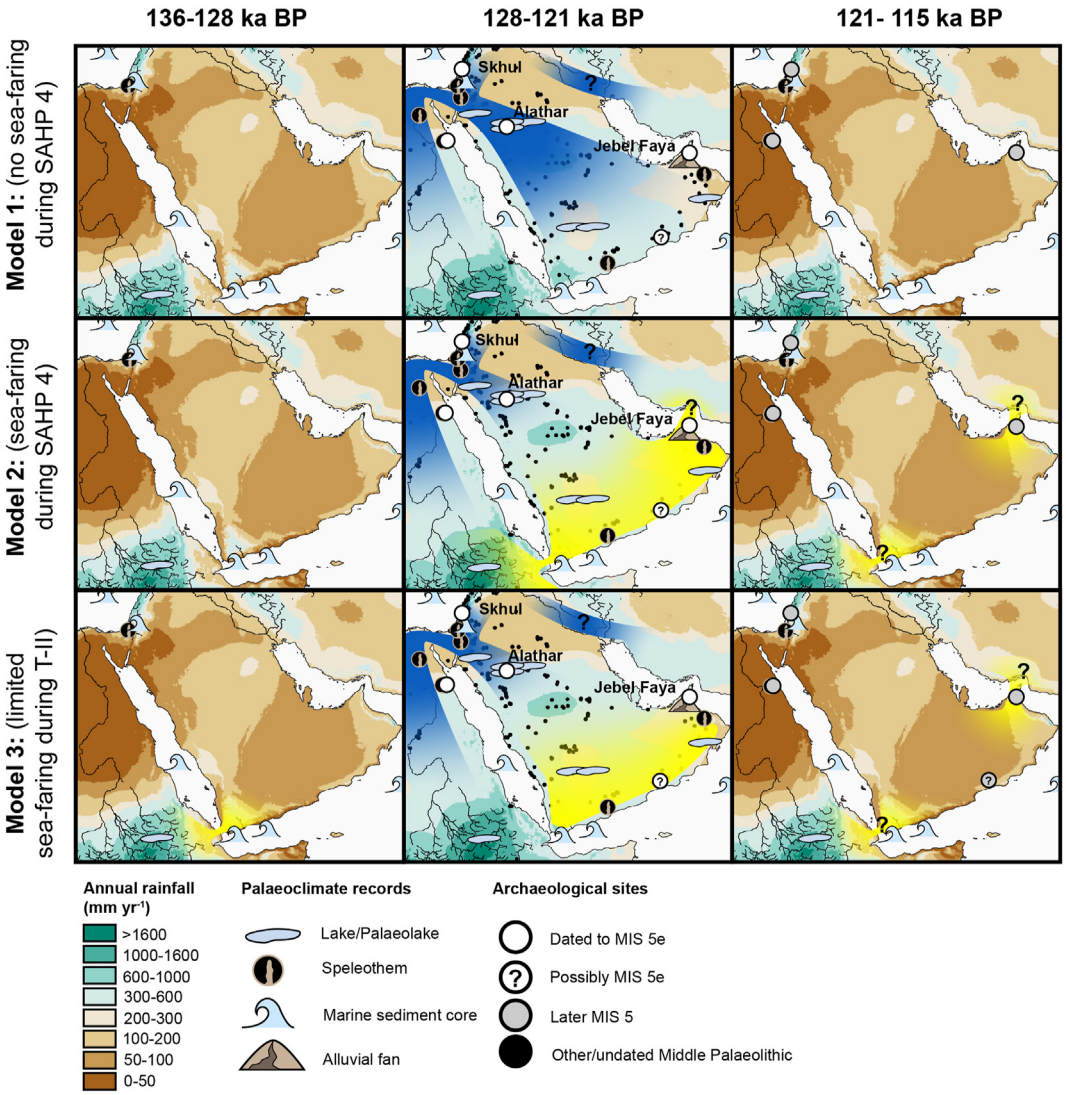

Fig. 4. Conceptual illustration of models for *H. sapiens* populations dispersals between 135–121 ka BP over northern (blue) and southern (yellow) routes. Rainfall maps include simulations for 140–120 ka BP (Otto-Bliesner, 2006) and the present-day (Fick and Hijmans, 2017) and are tuned to the chronology of Y99. All three models assume that the Sinai Peninsula (northern-route) was also a likely entry point into Arabia (supported by the assessment of archaeological assemblages from NE Africa, the Levant and northern Arabia). MIS 5e archaeological sites include the Alathar footprints (Saudi Arabia; Stewart et al., 2020a), Jebel Faya (Oman; Armitage et al., 2011), Skhul (Israel; Millard, 2008), Sodmein Cave (Egypt; Schmidt et al., 2015), and possibly Aybut al Awal (Oman; Rose et al., 2011). Undated/other Middle Palaeolithic sites were collated from (Groucutt et al., 2015b). Palaeoclimate records showing evidence of increased regional rainfall during MIS 5e include speleothems from Mukalla Cave (Yemen; this study), Hoti Cave (Oman; Burns et al., 2001; Fleitmann et al., 2003a, 2011), Soreq Cave and Negev Desert caves (Israel; Bar-Matthews et al., 2003; Vaks et al., 2006, 2010), and Wadi-Sannur Cave and Saqia Cave (El-Shenawy et al., 2018; Henselowsky et al., 2021); Palaeolakes Mundafan, Khujaymah, Jubbah, Alathar, Khall Amaysham, B'r Hayzan and Ti's al Ghada (Saudi Arabia; Petraglia et al., 2011, 2012; Rosenberg et al., 2011, 2013; Stewart et al., 2020b), Saiwan (Oman; Rosenberg et al., 2012), Lake Tana (Ethiopia; Lamb et al., 2018), and Mudawwara (Jordan; Petit-Maire et al., 2010); Marine records KL-15 and RC09-166 (Gulf of Aden; Fleitmann, 1997; Tierney et al., 2017), ODP 721/722 (Arabian Sea; Clark et al., 1997), KL-11 (Red Sea; Fleitmann, 1997; Siddall et al., 2003); ODP 967 (Mediterranean Sea; Larrasoana et al., 2003; Grant et al., 2017), and DSDDP (Dead Sea; Torfstein et al., 2015). Dispersal "routes" are non-directional to account for possible back-dispersals and perhaps southwards *H. sapiens* dispersals from the Levant. (For interpretation of the references to colour in this figure legend, the reader is referred to the Web version of this article.)

Bab-al-Mandab Strait was >26 km, similar or even wider than today. Even given the age uncertainties of the Y99 StalAge model and associated tie-points of the RSL (Grant et al., 2014, Fig. 3), the onset of Y99 growth lagged sea-level rise. Furthermore, at the end of SAHP 4 (121.170 ± 0.500 ka BP), sea-level was only 14.7 ± 3.1 m lower than today, yet the Bab-al-Mandab was ~20 km wide and remained a major obstacle to dispersal.

The observed time lag between sea-level rise and the onset of pluvial conditions in Arabia is consistent with a growing body of evidence for a decoupling of monsoon intensification and rising low-latitude insolation during T-II. Low-latitude insolation is a key control on the interhemispheric pressure gradient (iHPG), which regulates the intensity and position of the monsoon domain (e.g., Beck et al., 2018). Yet, despite rising insolation throughout T-II, our data, as well as previously published records from Sanbao (Cheng et al., 2009) and Soreq (Bar-Matthews et al., 2003; Grant et al., 2012, 2016; Häuselmann et al., 2015) caves, indicate that monsoon intensification did not occur until ~129–128 ka BP. This time lag can be related to the effects of the cold northern hemisphere conditions during HS11 (~135–130 ka BP). HS11 punctuated the warming of T-II and coincides with a major deglacial meltwater discharge (up to 0.3 Sv) phase into the North Atlantic (Marino et al., 2015). Meltwater discharge contributed to up to 70% of sea-level rise during T-II (Marino et al., 2015) and slowed, or maybe even

led to a collapse of AMOC (Böhm et al., 2015) leading to colder northern hemisphere temperatures. This reduced the iHPG, suppressed the effects of rising insolation, and inhibited the intensification of both the ASM/ISM and the EAM (Cheng et al., 2009; Häuselmann et al., 2015). Only once meltwater discharge and northern hemisphere temperatures stabilised at ~128 ka BP (Marino et al., 2015) could insolation have a full effect on the iHPG and permitted northward migration of the monsoon rainbelt. Thus, not only did high sea-levels act as a potential barrier to dispersal during MIS 5e, a supressed ASM/ISM throughout T-II meant that more arid conditions prevailed in Arabia and northeastern Africa when sea-levels were lower than today.

4. Models for *H. sapiens* dispersals across the southern-route

With a present-day width of ~26 km, the Bab-al-Mandab would represent a major obstacle for *H. sapiens* dispersals. A common suggestion is that a reduced width of the Strait facilitated a maritime crossing during T-II (Armitage et al., 2011; Bae et al., 2017; Beyer et al., 2021). However, the Y99 record indicates that the intensification of the monsoon and formation of grassland environments lagged sea-level rise and instead occurred once BaM_{width} had reached its Late Pleistocene maximum. This lag has potentially important implications for understanding both the route of *H. sapiens* dispersals and the cognitive, behavioural and technological capacities they possessed. Here, we provide three, not necessarily mutually exclusive, potential models for human dispersals throughout T-II and SAHP 4 (Fig. 4):

1) Dispersal occurred via a northern land-route during favourable conditions across Saharo-Arabia occurred between 128–121 ka BP and followed palaeohydrological corridors into Arabia and the Levant (Breeze et al., 2016; Nicholson et al., 2021).
2) A maritime dispersal via the southern-route occurred when sea-levels were high, but climates were favourable between 128–121 ka BP.
3) A maritime dispersal via the southern-route occurred prior to the onset of favourable climatic and environmental conditions at ~128 ka BP when sea-levels were lower (Armitage et al., 2011; Rohling et al., 2013).

Both model 2 and 3 require evidence of sea-faring, which is currently unknown prior to 65–50 ka BP (Norman et al., 2018), and model 3 assumes that *H. sapiens* were rather tolerant of arid and semi-arid conditions or exploited productive coastal environments (Erlandson and Braje, 2015). Previous findings, however, have linked occupations of the now Saharo-Arabian deserts interiors to wetter phases of MIS 5, providing support for model 1. This model is supported by techno-cultural similarities of archaeological assemblages from northeast Africa, the Nafud Desert and the Levant (Groucutt et al., 2015b, 2019).

The validity of the southern dispersal route hypothesis is thus dependent on evidence of sea-faring prior to and during MIS 5e – which is currently absent between Africa and SE Asia – and/or flexible environmental tolerances of *H. sapiens*. Conversely, the northern-route into Arabia was a viable route throughout SAHP 4 and perhaps throughout much of MIS 5 (Henselowsky et al., 2021). Whether crossing the Bab-al-Mandab Strait was an additional route will require further archaeological investigation of coastal settings (e.g., Bailey et al., 2015) to establish unambiguous demographic links between both sides of the Strait and/or providing examples of the sea-faring capabilities prior to 65 ka. Additionally, future dispersal pathway modelling studies must synthesise climatic, environmental and other topographic factors (e.g., Groucutt, 2020), which might have various and counteracting effects, to understand the variations of *H. sapiens* palaeobiogeographies.

5. Conclusions

Overall, our results indicate that the onset of increased rainfall occurred at 127.7 ka BP, after maximum deglaciation and sea-level rise. Whereas aridity prevailed throughout T-II when sea-levels were lower, the Bab-al-Mandab was at its greatest width at the onset of SAHP 4. We observe a distinct phase-lag between sea-level rise and monsoon intensification from records close to one-another. Our findings have pertinent impacts for understanding (1) the timing of monsoon intensification relative to sea-level rise throughout T-II in the Horn of Africa and Southern Arabia; (2) the timings and geographies of *H. sapiens* dispersals during MIS 5e, and (3) the potential behavioural and technological capabilities of *H. sapiens* at the onset of the Late Pleistocene.

Author contributions

SN collected the isotope data, produced the age-depth model and acted as primary author for the paper under the supervision of RH, AGWP and DF. SB, AM and DF supplied and collected the study material. HSG contributed to and supervised paleoanthropological/archaeological interpretations. All authors were involved in the ongoing refinement of the manuscript.

Declaration of competing interest

The authors declare that they have no known competing financial interests or personal relationships that could have appeared to influence the work reported in this paper.

Acknowledgments, samples, and data

This work was supported by the AHRC South, West and Wales Doctoral Training Partnership (Grant AH/L503939/1) the Swiss National Science Foundation (Grant PP002-110554/1 to DF). The initial stable-isotope and ^{230}Th age data used to construct the age-model is available at Nicholson et al. (2020). Our original StalAge age-depth data and high-resolution isotope data are available at the PANGAEA data repository (Nicholson et al., 2020). We thank Ian Candy and one anonymous reviewer for their constructive comments.

Appendix A. Supplementary data

Supplementary data to this article can be found online at https://doi.org/10.1016/j.quascirev.2022.107378.

References

Amies, J.D., Rohling, E.J., Grant, K.M., Rodríguez-Sanz, L., Marino, G., 2019. Quantification of african monsoon runoff during last interglacial sapropel S5. Paleoceanogr. Paleoclimatol. 34, 1487–1516.
Armitage, S.J., Jasim, S.A., Marks, A.E., Parker, A.G., Usik, V.I., Uerpmann, H.P., 2011. The southern route "out of Africa": evidence for an early expansion of modern humans into Arabia. Science 331, 453–456.
Arvidson, R., Becker, R., Shanabrook, A., Luo, W., Sturchio, N., Sultan, M., Lotfy, Z., Mahmood, A.M., El Alfy, Z., 1994. Climatic, eustatic, and tectonic controls on Quaternary deposits and landforms, Red Sea Coast, Egypt. J. Geophys. Res. Solid Earth 99, 12175–12190.
Bae, C.J., Douka, K., Petraglia, M.D., 2017. On the origin of modern humans: asian perspectives. Science 358, eaai9067.
Bailey, G.N., Devès, M.H., Inglis, R.H., Meredith-Williams, M.G., Momber, G., Sakellariou, D., Sinclair, A.G.M., Rousakis, G., Al Ghamdi, S., Alsharekh, A.M., 2015. Blue Arabia: Palaeolithic and underwater survey in SW Saudi Arabia and the role of coasts in Pleistocene dispersals. Quat. Int. 382, 42–57.
Bar-Matthews, M., Ayalon, A., Gilmour, M., Matthews, A., Hawkesworth, C.J., 2003. Sea - land oxygen isotopic relationships from planktonic foraminifera and

speleothems in the Eastern Mediterranean region and their implication for paleorainfall during interglacial intervals. Geochem. Cosmochim. Acta 67, 3181–3199.
Beck, J.W., Zhou, W., Li, C., Wu, Z., White, L., Xian, F., Kong, X., An, Z., 2018. A 550,000-year record of East Asian monsoon rainfall from 10Be in loess. Science 360, 877–881.
Berger, A., Loutre, M.F., 1991. Insolation values for the climate of the last 10 million years. Quat. Sci. Rev. 10, 297–317.
Berger, A., Loutre, M.F., 1999. Parameters of the Earths orbit for the last 5 Million years in 1 kyr resolution. Supplement to: berger, A; Loutre, M F (1991): insolation values for the climate of the last 10 million of years. Quat. Sci. Rev. 10 (4), 297–317. https://doi.org/10.1016/0277-3791(91)90033-Q.
Beyer, R.M., Krapp, M., Eriksson, A., Manica, A., 2021. Climatic windows for human migration out of Africa in the past 300,000 years. Nat. Commun. 12, 4889.
Böhm, E., Lippold, J., Gutjahr, M., Frank, M., Blaser, P., Antz, B., Fohlmeister, J., Frank, N., Andersen, M.B., Deininger, M., 2015. Strong and deep Atlantic meridional overturning circulation during the last glacial cycle. Nature 517, 73–76.
Breeze, P.S., Groucutt, H.S., Drake, N.A., White, T.S., Jennings, R.P., Petraglia, M.D., 2016. Palaeohydrological corridors for hominin dispersals in the Middle East ~250-70,000 years ago. Quat. Sci. Rev. 144, 155–185.
Bretzke, K., Armitage, S.J., Parker, A.G., Walkington, H., Uerpmann, H.P., 2013. The environmental context of paleolithic settlement at Jebel Faya, emirate sharjah, UAE. Quat. Int. 300, 83–93.
Burns, S.J., Fleitmann, D., Matter, A., Neff, U., Mangini, A., 2001. Speleothem evidence from Oman for continental pluvial events during interglacial periods. Geology 29, 623–626.
Cheng, H., Edwards, R.L., Broecker, W.S., Denton, G.H., Kong, X., Wang, Y., Zhang, R., Wang, X., 2009. Ice age terminations. Science 326, 248–252.
Cheng, H., Edwards, R.L., Sinha, A., Spötl, C., Yi, L., Chen, S., Kelly, M., Kathayat, G., Wang, X., Li, X., Kong, X., Wang, Y., Ning, Y., Zhang, H., 2016. The Asian monsoon over the past 640,000 years and ice age terminations. Nature 534, 640–646.
Clark, I., Fritz, P., 1997. Environmnetal Istopes in Hydrogeology Lewis Publishers, New York. deMenocal, P.B., 1995. Plio-pleistocene african climate. Science 270, 53–59.
El-Shenawy, M.I., Kim, S.-T., Schwarcz, H.P., Asmerom, Y., Polyak, V.J., 2018. Speleothem evidence for the greening of the Sahara and its implications for the early human dispersal out of sub-Saharan Africa. Quat. Sci. Rev. 188, 67–76.
Erlandson, J.M., Braje, T.J., 2015. Coasting out of Africa: the potential of mangrove forests and marine habitats to facilitate human coastal expansion via the Southern Dispersal Route. Quat. Int. 382, 31–41.
Fick, S.E., Hijmans, R.J., 2017. WorldClim 2: new 1-km spatial resolution climate surfaces for global land areas. Int. J. Climatol. 37, 4302–4315.
Fleitmann, D., 1997. Klastischer Eintrag in das Rote Meer und den Golf von Aden durch den Arabischen Monsun-Untersuchungen an Kolbenlot-Kernen. Masters thesis Diplom-Arbeit, Institut und Museum für Geologie und Paläontologie der Georg-August-Universität zu Göttingen.
Fleitmann, D., Burns, S.J., Mangini, A., Mudelsee, M., Kramers, J., Villa, I., Neff, U., Al-Subbary, A.A., Buettner, A., Hippler, D., Matter, A., 2007. Holocene ITCZ and Indian monsoon dynamics recorded in stalagmites from Oman and Yemen (Socotra). Quat. Sci. Rev. 26, 170–188.
Fleitmann, D., Burns, S.J., Mudelsee, M., Neff, U., Kramers, J., Mangini, A., Matter, A., 2003a. Holocene forcing of the Indian monsoon recorded in a stalagmite from Southern Oman. Science 300, 1737–1739.
Fleitmann, D., Burns, S.J., Neff, U., Mangini, A., Matter, A., 2003b. Changing moisture sources over the last 330,000 years in Northern Oman from fluid-inclusion evidence in speleothems. Qua. Res. 60, 223–232.
Fleitmann, D., Burns, S.J., Neff, U., Mudelsee, M., Mangini, A., Matter, A., 2004. Palaeoclimatic interpretation of high-resolution oxygen isotope profiles derived from annually laminated speleothems from Southern Oman. Quat. Sci. Rev. 23, 935–945.
Fleitmann, D., Burns, S.J., Pekala, M., Mangini, A., Al-Subbary, A., Al-Aowah, M., Kramers, J., Matter, A., 2011. Holocene and Pleistocene pluvial periods in Yemen, southern Arabia. Quat. Sci. Rev. 30, 783–787.
GEBCO Compilation Group, 2020. GEBCO 2020 Grid.
Gierz, P., Werner, M., Lohmann, G., 2017. Simulating climate and stable water isotopes during the Last Interglacial using a coupled climate-isotope model. J. Adv. Model. Earth Syst. 9, 2027–2045.
Grant, K.M., Grimm, R., Mikolajewicz, U., Marino, G., Ziegler, M., Rohling, E.J., 2016. The timing of Mediterranean sapropel deposition relative to insolation, sea-level and African monsoon changes. Quat. Sci. Rev. 140, 125–141.
Grant, K.M., Rohling, E.J., Bar-Matthews, M., Ayalon, A., Medina-Elizalde, M., Ramsey, C.B., Satow, C., Roberts, A.P., 2012. Rapid coupling between ice volume and polar temperature over the past 50,000 years. Nature 491, 744–747.
Grant, K.M., Rohling, E.J., Ramsey, C.B., Cheng, H., Edwards, R.L., Florindo, F., Heslop, D., Marra, F., Roberts, A.P., Tamisiea, M.E., Williams, F., 2014. Sea-level variability over five glacial cycles. Nat. Commun. 5, 5076.
Grant, K.M., Rohling, E.J., Westerhold, T., Zabel, M., Heslop, D., Konijnendijk, T., Lourens, L., 2017. A 3 million year index for North African humidity/aridity and the implication of potential pan-African Humid periods. Quat. Sci. Rev. 171, 100–118.
Groucutt, H.S., 2020. Volcanism and human prehistory in Arabia. J. Volcanol. Geoth. Res. 402, 107003.
Groucutt, H.S., Grün, R., Zalmout, I.A.S., Drake, N.A., Armitage, S.J., Candy, I., Clark-Wilson, R., Louys, J., Breeze, P.S., Duval, M., Buck, L.T., Kivell, T.L., Pomeroy, E., Stephens, N.B., Stock, J.T., Stewart, M., Price, G.J., Kinsley, L., Sung, W.W., Alsharekh, A., Al-Omari, A., Zahir, M., Memesh, A.M., Abdulshakoor, A.J., Al-Masari, A.M., Bahameem, A.A., Al Murayyi, K.M.S., Zahrani, B., Scerri, E.M.L., Petraglia, M.D., 2018. Homo sapiens in Arabia by 85,000 years ago. Nat. Ecol. Evolu. 2, 800–809.
Groucutt, H.S., Petraglia, M.D., Bailey, G., Scerri, E.M.L., Parton, A., Clark-Balzan, L., Jennings, R.P., Lewis, L., Blinkhorn, J., Drake, N.A., Breeze, P.S., Inglis, R.H., Devès, M.H., Meredith-Williams, M., Boivin, N., Thomas, M.G., Scally, A., 2015a. Rethinking the dispersal of Homo sapiens out of Africa. Evol. Anthropol. 24, 149–164.
Groucutt, H.S., Scerri, E.M.L., Lewis, L., Clark-Balzan, L., Blinkhorn, J., Jennings, R.P., Parton, A., Petraglia, M.D., 2015b. Stone tool assemblages and models for the dispersal of Homo sapiens out of Africa. Quat. Int. 382, 8–30.
Groucutt, H.S., Scerri, E.M.L., Stringer, C., Petraglia, M.D., 2019. Skhul lithic technology and the dispersal of Homo sapiens into Southwest Asia. Quat. Int. 515, 30–52.
Groucutt, H.S., White, T.S., Clark-Balzan, L., Parton, A., Crassard, R., Shipton, C., Jennings, R.P., Parker, A.G., Breeze, P.S., Scerri, E.M.L., Alsharekh, A., Petraglia, M.D., 2015c. Human occupation of the arabian empty quarter during MIS 5: evidence from mundafan Al-buhayrah, Saudi Arabia. Quat. Sci. Rev. 119, 116–135.
Häuselmann, A.D., Fleitmann, D., Cheng, H., Tabersky, D., Günther, D., Edwards, R.L., 2015. Timing and nature of the penultimate deglaciation in a high alpine stalagmite from Switzerland. Quat. Sci. Rev. 126, 264–275.
Henselowsky, F., Eichstädter, R., Schröder-Ritzrau, A., Herwartz, D., Almoazamy, A., Frank, N., Kindermann, K., Bubenzer, O., 2021. Speleothem growth phases in the central Eastern Desert of Egypt reveal enhanced humidity throughout MIS 5. Quat. Int.
Herold, M., Lohmann, G., 2009. Eemian tropical and subtropical African moisture transport: an isotope modelling study. Clim. Dynam. 33, 1075–1088.
Jennings, R.P., Shipton, C., Breeze, P., Cuthbertson, P., Bernal, M.A., Wedage, W.M.C.O., Drake, N.A., White, T.S., Groucutt, H.S., Parton, A., Clark-Balzan, L., Stimpson, C., al Omari, A.A., Alsharekh, A., Petraglia, M.D., 2015. Multi-scale Acheulean landscape survey in the Arabian Desert. Quat. Int. 382, 58–81.
Lamb, H.F., Bates, C.R., Bryant, C.L., Davies, S.J., Huws, D.G., Marshall, M.H., Roberts, H.M., 2018. 150,000-year palaeoclimate record from northern Ethiopia supports early, multiple dispersals of modern humans from Africa. Sci. Rep. 8.
Lambeck, K., Purcell, A., Flemming, N.C., Vita-Finzi, C., Alsharekh, A.M., Bailey, G.N., 2011. Sea level and shoreline reconstructions for the Red Sea: isostatic and tectonic considerations and implications for hominin migration out of Africa. Quat. Sci. Rev. 30, 3542–3574.
Larrasoaña, J.C., Roberts, A.P., Rohling, E.J., 2013. Dynamics of green sahara periods and their role in hominin evolution. PLoS One 8, e76514.
Larrasoana, J.C., Roberts, A.P., Rohling, E.J., Winklhofer, M., Wehausen, R., 2003. Three million years of monsoon variability over the northern Sahara. Clim. Dynam. 21, 689–698.
Lisiecki, L.E., Raymo, M.E., 2005. A Pliocene-Pleistocene stack of 57 globally distributed benthic δ 18O records. Paleoceanography 20, 1–17.
Marino, G., Rohling, E.J., Rodríguez-Sanz, L., Grant, K.M., Heslop, D., Roberts, A.P., Stanford, J.D., Yu, J., 2015. Bipolar seesaw control on last interglacial sea level. Nature 522, 197–201.
McLaren, S.J., Al-Juaidi, F., Bateman, M.D., Millington, A.C., 2009. First evidence for episodic flooding events in the arid interior of central Saudi Arabia over the last 60 ka. J. Quat. Sci. 24, 198–207.
Mellars, P., Gori, K.C., Carr, M., Soares, P.A., Richards, M.B., 2013. Genetic and archaeological perspectives on the initial modern human colonization of southern Asia. Proc. Natl. Acad. Sci. Unit. States Am. 110, 10699–10704.
Menviel, L., Govin, A., Avenas, A., Meissner, K.J., Grant, K.M., Tzedakis, P.C., 2021. Drivers of the evolution and amplitude of african humid periods. Commun. Earth Environ. 2, 237.
Millard, A.R., 2008. A critique of the chronometric evidence for hominid fossils: I. Africa and the Near East 500-50 ka. J. Hum. Evol. 54, 848–847.
Nicholson, S.L., Hosfield, R., Groucutt, H.S., Pike, A.W.G., Burns, S.J., Matter, A., Fletimann, D.. https://doi.pangaea.de/10.1594/PANGAEA.924793.
Nicholson, S.L., Hosfield, R., Groucutt, H.S., Pike, A.W.G., Fleitmann, D., 2021. Beyond arrows on a map: the dynamics of Homo sapiens dispersal and occupation of Arabia during Marine Isotope Stage 5. J. Anthropol. Archaeol. 62, 101269.
Nicholson, S.L., Pike, A.W.G., Hosfield, R., Roberts, N., Sahy, D., Woodhead, J., Cheng, H., Edwards, R.L., Affolter, S., Leuenberger, M., Burns, S.J., Matter, A., Fleitmann, D., 2020. Pluvial periods in Southern Arabia over the last 1.1 million-years. Quat. Sci. Rev. 229, 106112.
Norman, K., Inglis, J., Clarkson, C., Faith, J.T., Shulmeister, J., Harris, D., 2018. An early colonisation pathway into northwest Australia 70-60,000 years ago. Quat. Sci. Rev. 180, 229–239.
Otto-Bliesner, B.L., 2006. Simulating arctic climate warmth and icefield retreat in the last interglaciation. Science 311, 1751–1753.
Parton, A., Clark-Balzan, L., Parker, A.G., Preston, G.W., Sung, W.W., Breeze, P.S., Leng, M.J., Groucutt, H.S., White, T.S., Alsharekh, A., Petraglia, M.D., 2018. Middle-late quaternary palaeoclimate variability from lake and wetland deposits in the Nefud Desert, Northern Arabia. Quat. Sci. Rev. 202, 78–97.
Parton, A., Farrant, A.R., Leng, M.J., Schwenninger, J.L., Rose, J.I., Uerpmann, H.P., Parker, A.G., 2013. An early MIS 3 pluvial phase in Southeast Arabia: climatic and archaeological implications. Quat. Int. 300, 62–74.
Parton, A., Farrant, A.R., Leng, M.J., Telfer, M.W., Groucutt, H.S., Petraglia, M.D.,

Parker, A.G., 2015a. Alluvial fan records from southeast Arabia reveal multiple windows for human dispersal. Geology 43, 295–298.
Parton, A., White, T.S., Parker, A.G., Breeze, P.S., Jennings, R., Groucutt, H.S., Petraglia, M.D., 2015b. Orbital-scale climate variability in Arabia as a potential motor for human dispersals. Quat. Int. 382, 82–97.
Petit-Maire, N., Carbonel, P., Reyss, J.L., Sanlaville, P., Abed, A.M., Bourrouilh, R., Fontugne, M.R., Yasin, S., 2010. A vast Eemian palaeolake in Southern Jordan (29°N). Global Planet. Change 72, 368–373.
Petraglia, M.D., Alsharekh, A., Breeze, P., Clarkson, C., Crassard, R., Drake, N.A., Groucutt, H.S., Jennings, R.P., Parker, A.G., Parton, A., Roberts, R.G., Shipton, C., Matheson, C., Al-Omari, A., Veall, M.A., 2012. Hominin dispersal into the nefud Desert and Middle palaeolithic settlement along the Jubbah palaeolake, northern Arabia. PLoS One 7, e49840.
Petraglia, M.D., Alsharekh, A.M., Crassard, R., Drake, N.A., Groucutt, H., Parker, A.G., Roberts, R.G., 2011. Middle paleolithic occupation on a marine isotope stage 5 lakeshore in the nefud desert, Saudi Arabia. Quat. Sci. Rev. 30, 1555–1559.
Petraglia, M.D., Breeze, P.S., Groucutt, H.S., 2019. Blue Arabia, green Arabia: examining human colonisation and dispersal models. In: Rasul, N.M.A., Stewart, I.C.F. (Eds.), Geological Setting, Palaeoenvironment and Archaeology of the Red Sea. Springer International Publishing, Cham, pp. 675–683.
Petraglia, M.D., Parton, A., Groucutt, H.S., Alsharekh, A., 2015. Green Arabia: human prehistory at the crossroads of continents. Quat. Int. 382, 1–7.
Rohling, E.J., Grant, K., Bolshaw, M., Roberts, A.P., Siddall, M., Hemleben, C., Kucera, M., 2009. Antarctic temperature and global sea level closely coupled over the past five glacial cycles. Nat. Geosci. 2, 500–504.
Rohling, E.J., Grant, K., Hemleben, C., Siddall, M., Hoogakker, B.A.A., Bolshaw, M., Kucera, M., 2008. High rates of sea-level rise during the last interglacial period. Nat. Geosci. 1, 38–42.
Rohling, E.J., Grant, K.M., Roberts, A.P., Larrasoaña, J.-C., 2013. Paleoclimate variability in the mediterranean and Red Sea regions during the last 500,000 years. Curr. Anthropol. 54, S183–S201.
Rohling, E.J., Marino, G., Grant, K.M., 2015. Mediterranean climate and oceanography, and the periodic development of anoxic events (sapropels). Earth Sci. Rev. 143, 62–97.
Rose, J.I., Usik, V.I., Marks, A.E., Hilbert, Y.H., Galletti, C.S., Parton, A., Geiling, J.M., Černý, V., Morley, M.W., Roberts, R.G., 2011. The nubian complex of dhofar, Oman: an african Middle stone age industry in southern Arabia. PLoS One 6, e28239.
Rosenberg, T.M., Preusser, F., Blechschmidt, I., Fleitmann, D., Jagher, R., Matter, A., 2012. Late Pleistocene palaeolake in the interior of Oman: a potential key area for the dispersal of anatomically modern humans out-of-Africa? J. Quat. Sci. 27, 13–16.
Rosenberg, T.M., Preusser, F., Fleitmann, D., Schwalb, A., Penkman, K.E.H., Schmid, T.W., Al-Shanti, M.A., Kadi, K.A., Matter, A., 2011. Humid periods in southern Arabia: windows of opportunity for modern human dispersal. Geology 39, 1115–1118.
Rosenberg, T.M., Preusser, F., Risberg, J., Plikk, A., Kadi, K.A., Matter, A., Fleitmann, D., 2013. Middle and Late Pleistocene humid periods recorded in palaeolake deposits of the Nafud desert, Saudi Arabia. Quat. Sci. Rev. 70, 109–123.
Schmidt, C., Kindermann, K., van Peer, P., Bubenzer, O., 2015. Multi-emission luminescence dating of heated chert from the Middle stone age sequence at Sodmein cave (Red Sea mountains, Egypt). J. Archaeol. Sci. 63, 94–103.
Siddall, M., Rohling, E.J., Almogi-Labin, A., Hemleben, C., Meischner, D., Schmelzer, I., Smeed, D.A., 2003. Sea-level fluctuations during the last glacial cycle. Nature 423, 853–858.
Stewart, M., Clark-Wilson, R., Breeze, P.S., Janulis, K., Candy, I., Armitage, S.J., Ryves, D.B., Louys, J., Duval, M., Price, G.J., Cuthbertson, P., Bernal, M.A., Drake, N.A., Alsharekh, A.M., Zahrani, B., Al-Omari, A., Roberts, P., Groucutt, H.S., Petraglia, M.D., 2020a. Human footprints provide snapshot of last interglacial ecology in the Arabian interior. Sci. Adv. 6, eaba8940.
Stewart, M., Louys, J., Breeze, P.S., Clark-Wilson, R., Drake, N.A., Scerri, E.M.L., Zalmout, I.S., Al-Mufarreh, Y.S.A., Soubhi, S.A., Haptari, M.A., Alsharekh, A.M., Groucutt, H.S., Petraglia, M.D., 2020b. A taxonomic and taphonomic study of Pleistocene fossil deposits from the western Nefud Desert, Saudi Arabia. Qua. Res. 95, 1–22.
Tierney, J.E., deMenocal, P.B., Zander, P.D., 2017. A climatic context for the out-of-Africa migration. Geology 45, 1023–1026.
Torfstein, A., Goldstein, S.L., Kushnir, Y., Enzel, Y., Haug, G., Stein, M., 2015. Dead Sea drawdown and monsoonal impacts in the Levant during the last interglacial. Earth Planet Sci. Lett. 412, 235–244.
Vaks, A., Bar-Matthews, M., Ayalon, A., Matthews, A., Frumkin, A., Dayan, U., Halicz, L., Almogi-Labin, A., Schilman, B., 2006. Paleoclimate and location of the border between Mediterranean climate region and the Saharo-Arabian Desert as revealed by speleothems from the northern Negev Desert, Israel. Earth Planet Sci. Lett. 249, 384–399.
Vaks, A., Bar-Matthews, M., Matthews, A., Ayalon, A., Frumkin, A., 2010. Middle-late quaternary paleoclimate of northern margins of the saharan-Arabian desert: reconstruction from speleothems of Negev Desert, Israel. Quat. Sci. Rev. 29, 2647–2662.
Weldeab, S., Lea, D.W., Schneider, R.R., Andersen, N., 2007. 155,000 Years of west african monsoon and ocean thermal evolution. Science 316, 1303–1307.